Materials and Design 56 (2014) 629–634

Contents lists available at ScienceDirect

Materials and Design

journal homepage: www.elsevier.com/locate/matdes

Fabrication of Ti–Nb–Ag alloy via powder metallurgy for biomedical applications

Ming Wen [a,b], Cuie Wen [c], Peter Hodgson [a], Yuncang Li [a,*]

[a] Institute for Frontier Materials, Deakin University, Geelong, Victoria 3217, Australia
[b] Kunming Institute of Precious Metals, Kunming, Yunnan 650106, China
[c] Faculty of Engineering and Industrial Sciences, Swinburne University of Technology, Hawthorn, Victoria 3122, Australia

ARTICLE INFO

Article history:
Received 23 May 2013
Accepted 26 November 2013
Available online 4 December 2013

Keywords:
Ti–Nb–Ag alloy
Spark plasma sintering
Vacuum sintering
Microstructure
Mechanical properties

ABSTRACT

Ti and some of its alloys are widely used as orthopedic implants. In the present study, Ti–26Nb–5Ag alloys were prepared by mechanical alloying followed by vacuum furnace sintering or spark plasma sintering (SPS). The microstructure and mechanical properties of the Ti–Nb–Ag alloys were investigated using X-ray diffraction (XRD), scanning electron microscopy (SEM) combined with energy-dispersive X-ray spectroscopy (EDX), compressive and micro-hardness tests. The effect of different sintering methods on the microstructure and properties of Ti–Nb–Ag alloy was discussed. The results showed that the titanium alloy sintered by vacuum furnace exhibited a microstructure consisting of α, β and a small amount of α″ martensite phase; whilst the SPS sintered alloy exhibited a microstructure consisting of α, β and a small amount of α″ martensite phase, as well as a nanostructured Ag homogeneously distributed at the boundaries of the β phases. The Ti–Nb–Ag alloy sintered by SPS possessed fracture strength nearly 3 times of the alloy sintered by vacuum furnace.

1. Introduction

Titanium (Ti) and some Ti alloys have been widely used in the biomedical field due to their lower modulus, superior biocompatibility and excellent corrosion resistance compared to stainless steels and Co–Cr alloys [1,2]. Currently, commercially pure (CP) Ti and Ti–6Al–4V are the most commonly used implant materials. However, it has been reported that Ti–6Al–4V may not be appropriate in the human body as Al and V are toxic and could have the potential to cause a series of ailments including Alzheimer's disease [3,4]. Recently, it has been reported that Ti–Nb alloys exhibit complete biocompatibility [5,6]. In particular, the Ti-26 at.% alloy possesses excellent shape memory effect and super-elasticity after thermomechanical treatments [7].

Surgical implant procedures, such as partial or total joint arthroplasty, are commonly undertaken to restore joint function in affected patients, but one of the limitations associated with total joint arthroplasty is that the implant has associated infections, which accounts for an enormous medical cost, an increase in morbidity and a decrease in patient satisfaction. Silver (Ag) has been known to have a disinfecting effect for a long time, and has found applications in traditional medicines and culinary items. Nanostructured Ag has been reported to exhibit excellent antimicrobial properties [8]. It is generally accepted that the high affinity of Ag toward sulphur or phosphorus found in abundance throughout the cell membrane is the key element of the antibacterial property since nanostructured Ag can react with sulphur-containing proteins inside or outside the cell membrane and thus affect bacterial cell viability [9,10]. Due to these unique properties, it can be envisaged that Ti alloys with an addition of Ag can find extended usages in biomedical applications. Moreover, it is anticipated that Ti alloys with a microstructure dispersed with nanostructured Ag may exhibit antibacterial function. Thus an appropriate fabrication method to produce such kind of Ti alloys is highly desired.

Spark plasma sintering (SPS) is a novel materials processing technique with a unique combination of amperage and pressure in sintering. It can be used for the rapid densification of powdered metal alloys, intermetallics, ceramics and composites within a few minutes and at significantly reduced temperature compared to conventional sintering, making it particularly useful for the manufacturing of metal materials with refined grain structures or nanoscale structures [11,12]. In the present study, Ti–26Nb–5Ag alloys were fabricated via powder metallurgy. Ball milling was used for mixing the Ti, Nb and Ag. Then a vacuum furnace and a spark plasma sintering (SPS) machine were used to sinter the alloys, respectively. The microstructure and mechanical properties of the Ti–Nb–Ag alloys sintered by both vacuum furnace and SPS were comparatively investigated using XRD and SEM with element mapping technique.

* Corresponding author. Tel.: +61 3 52272168; fax: +61 3 52271103.
E-mail address: yuncang.li@deakin.edu.au (Y. Li).

0261-3069/$ - see front matter © 2013 Elsevier Ltd. All rights reserved.
http://dx.doi.org/10.1016/j.matdes.2013.11.066

2. Method

Commercially available elemental powders of Ti, niobium (Nb) (Atlantic Equipment Engineers, ⩽45 μm), and Ag (Sigma–Aldrich, 5–8 μm) were used as starting materials. The elemental metal powders were blended together to yield a nominal composition of Ti–26Nb–5Ag (atomic percent hereafter). A Retsch planetary ball mill with stainless steel balls (10 mm diameter) were used for the mechanical alloying. The ball milling was carried out at a ball to powder ratio of 10:1 and a rotation rate of 200 rpm for 20 h in an argon atmosphere. The powders after ball milling for 20 h were processed via 2 routes. The first route was the vacuum sintering process. The ball milled powders were compacted under a pressure of 160 MPa and then sintered in a vacuum furnace at a temperature of 1000 °C for 5 h. The samples were cooled in furnace and taken out when the temperature was below 100 °C. The second route was the SPS process. The ball milled powders were placed in a graphite die and sintered using an SPS system (SPS SYNTEX, Japan). The sintering was carried out at 1000 °C for 5 min at a preheating rate of 6000 °C/h. Then the samples were cooled down to room temperature at a cooling rate of 2000 °C/h.

The phases of the samples were characterized using an X-ray diffractometer (XRD) with Cu Kα radiation (Panalytical X'Pert Pro). A field emission scanning electron microscope (FE-SEM, Supra 55VP) was used to observe the powder morphologies and microstructures. The chemical composition of the ball milled powders and the samples after sintering were investigated using scanning electron microscopy combined with energy-dispersive X-ray spectroscopy (SEM–EDX). The microhardness of sintered samples was measured using a Vickers hardness tester (FM-700, Future-Tech) with a load of 100 g and a dwell time of 10 s. The Ti alloy samples were ground using silicon carbide papers, and polished by oxide polishing suspensions (OPS) before SEM observation and Vickers hardness testing. The mechanical properties were evaluated by compression tests using a Material Testing System (Shimadzu, AG–IC, 100 KN) at a strain rate of 6×10^{-4} s^{-1}. The fracture surface was observed using SEM.

3. Results and discussions

Fig. 1 presents the morphologies of as-received powders and ball-milled Ti–Nb–Ag powders. It can be seen that initial Ti (Fig. 1a), Nb (Fig. 1b) and Ag (Fig. 1c) powders were irregularly shaped. The particle size of Ti varied from 4.6 to 29.3 μm with a mean particle size of 12.8 μm. The particle size of Nb varied from 0.7 to 52.4 μm with a mean particle size of 5.5 μm. Compared with the almost entirely disaggregated Ti and Nb powders, Ag powders showed remarkable aggregation which may be attributed to the small particle size (5–8 μm). The morphology of the Ti–Nb–Ag particles after ball milling for 20 h is shown in Fig. 1d. The particle size of the ball milled particles varied from 0.8 to 28.9 μm with a mean particle size of 5.7 μm. During ball milling process, the mixed powders underwent fracture and cold-welding processes repeatedly, with the ultimate development of an equiaxed morphology indicative of the dynamic equilibrium state of fracture and cold-welding. Additionally, EDX mapping was conducted to reveal the element distribution of the ball milled particles (Fig. 2). It can be seen that all of the elements (Ti, Nb and Ag) were homogeneously distributed in the whole area, suggesting an effective mechanical alloying of the elemental metal powders after 20 h of ball milling.

Fig. 3a shows the XRD patterns of the Ti–26Nb–5Ag powders before and after ball milling for 2 and 20 h. It can be seen that the intensity of diffraction peaks decreased and peaks became broaden after ball milling for 2 h. The peaks belonged to Ti, Nb, and Ag can still be assigned according to the initial peaks of elemental Ti, Nb, and Ag powders, respectively. The peak broadening was due to the decreasing of crystalline size and increasing of lattice micro-strain. As with the increasing of milling time, the peaks of the mixed powder became broaden and even vanish. Peak shift was observed with increasing milling time; the peak at 38.4° after 2 h was subsequently observed with significant broadening at 38.5° after 20 h of milling. However, following the extended milling, other peaks were difficult to discern. The peaks shift can be ascribed to the incorporation of Ti, Nb and Ag and thus the formation of metastable solid solution by mechanical alloying. Fig. 3b shows the XRD patterns of the Ti–Nb–Ag samples after vacuum sintering and SPS. It can be seen that the sample sintered by vacuum furnace was composed of α, β and a small amount of α″ martensite phases; by contrast, the sample sintered via SPS showed evidence of elemental Ag (1 1 0), Ag (2 0 0) and Ag (3 1 1) peaks in addition to the α, β, and α″ peaks. These results suggested that elemental Ag was formed during SPS due to the significantly enhanced heating rate and the unique spark plasma sintering mechanism.

Fig. 4 shows the SEM micrographs of Ti–26Nb–5Ag alloy after vacuum sintering. It can be seen that some pores existed in the

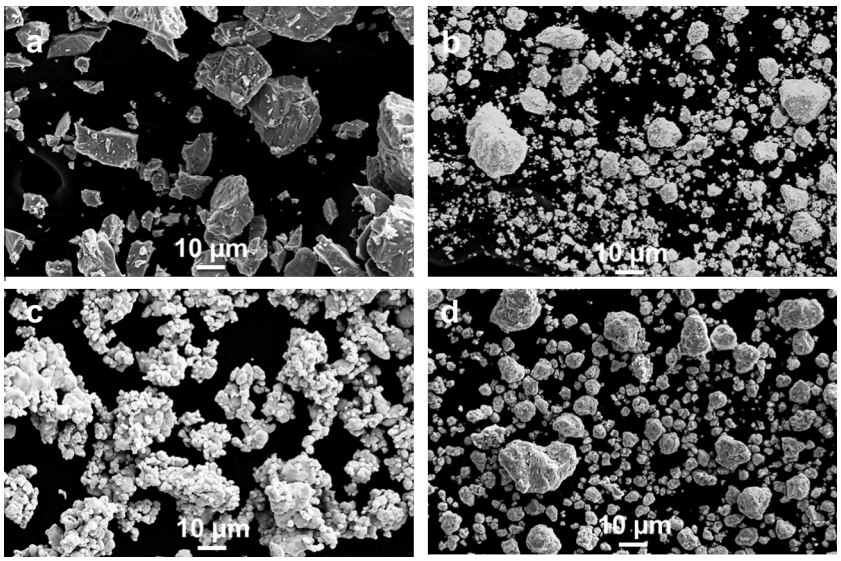

Fig. 1. The morphologies of powders: (a) Ti, (b) Nb, (c) Ag, and (d) Ti–26Nb–5Ag powder blends after ball milling for 20 h.